Maxwell's demon and Smoluchowski's trap door

Jianzhou Zheng,[1] Xiao Zheng,[1] Yang Zhao,[1,2,*] Yang Xie,[3] ChiYung Yam,[1] GuanHua Chen,[1,2,†]
Qing Jiang,[4] and Allen T. Chwang[5]
[1]*Department of Chemistry, University of Hong Kong, Hong Kong, China*
[2]*Center of Theoretical and Computational Physics, University of Hong Kong, Hong Kong, China*
[3]*Department of Physics, University of Hong Kong, Hong Kong, China*
[4]*Department of Mechanical Engineering, University of California, Riverside, California, USA*
[5]*Department of Mechanical Engineering, University of Hong Kong, Hong Kong, China*
(Received 30 August 2006; revised manuscript received 14 November 2006; published 17 April 2007; corrected 4 May 2007)

A simulation has been performed to reveal the detailed dynamics and statistical behavior of a Maxwell demon of the simplest kind, a trap door held over by a spring inside a box filled with gas molecules. The role of such a demon can be controlled by tuning Smoluchowski's fluctuations. When the demon is in thermal equilibrium with the rest of the system, it fails to function as designed, and when it is separately subjected to a thermal bath with a different temperature, it creates a temperature or density gradient between the two chambers of the box it divides. As a Maxwell demon, the trap-door device creates more readily a density gradient than that of temperature.

DOI: 10.1103/PhysRevE.75.041109 PACS number(s): 05.20.−y, 01.55.+b, 05.40.Jc, 05.70.−a

I. INTRODUCTION

In his 1871 book [1], *Theory of Heat*, Maxwell introduced the celebrated demon, in his own words, "… a being whose faculties are so sharpened that he can follow every molecule in its course, whose attributes are still as essentially finite as our own, would be able to do what is at present impossible to us." Thomson later nicknamed Maxwell's fictitious being of molecular size "Maxwell's intelligent demon" [2]. He stated that "the definition of a demon, is an intelligent being endowed with free will and fine enough tactile and perceptive organization to give him the faculty of observing and influencing individual molecules of matter." Maxwell introduced the demon to illustrate the statistical nature of the second law of thermodynamics. Subsequently, there have been many debates on whether such a demon exists and whether it would function as designed. Most recently, with the advent of nanomachinery devices, the prospect of testing fundamental hypotheses of thermodynamics and realizing Maxwell's demons at the nanoscale has been contemplated [3].

In 1912 Smoluchowski pointed out that thermal fluctuations would prevent any automatic device from operating successfully as a Maxwell demon in a lecture entitled "Experimentally Verifiable Molecular Phenomena that Contradict Ordinary Thermodynamics" [4]. Based on this, Feynman proposed the now-celebrated ratchet-and-pawl system and showed that no net work can be extracted from a single heat source using the ratchet and pawl [5]. In addition, he demonstrated that as soon as a second heat bath with a different temperature is introduced, the ratchet rotates clockwise or counterclockwise depending on the temperature difference between the two baths. Most of the investigations of Maxwell's demon have been thought experiments. Despite intense, lasting interest in Maxwell's demons and an incessant quest for them as documented in the literature, only a few microscopic simulations have been carried out to examine Maxwell's demons. Zhang and Zhang [6] formulated a set of sufficient conditions for the survival of a Maxwell's demon: (i) a device can be used to generate and sustain a robust momentum flow inside an isolated system, and (ii) a system with an invariant phase volume is capable of supporting such a flow. However, they provided no realistic models and simulations. In 1992 a trap-door device was studied for the first time via numerical simulation by Skordos and Zurek [7] showing that the trap door, acting only as a pump, cannot extract useful work from the thermal motion of the molecules. Skordos later [8] analyzed a membrane system and stated that the second law of thermodynamics requires the incompressibility of microscopic dynamics or an appropriate energy cost for compressible microscopic dynamics. Jarzynski and Mazonka [9] introduced a simple realization of Feynman's ratchet-and-pawl system and indicated that their model can act both as a heat engine and as a refrigerator. However, there is no molecular dynamics result to support their conclusion. Meurs and co-workers [10] have mentioned several models to show rectifications of thermal fluctuations, but only analytical results were presented. Other previous attempts include employing the overdamped Fokker-Planck equations with stochastic variables to simulate Feynman's ratchet and pawl [11] and modeling asymmetric Brownian particles immersed in thermal baths made of gaseous molecules that are treated explicitly [12]. The former overly simplifies the gas-particle dynamics, and the latter has no well-defined Maxwell's demon. To our knowledge, few realistic microscopic simulations have been systematically carried out to examine the detailed dynamics of Maxwell's demons.

Figure 1(a) depicts a trap door held over by a spring, a device termed by Feynman in his famous lecture notes as the simplest Maxwell demon [5]. Fast-moving molecules from the right chamber can come through because they are able to lift the trap door, and their slow-moving counterparts in the left chamber are bounced back. As time goes on, the particles in the left compartment will have a higher temperature (and a higher particle density) than that of the right, and the

*Electronic address: yang@yangtze.hku.hk
†Electronic address: ghc@everest.hku.hk

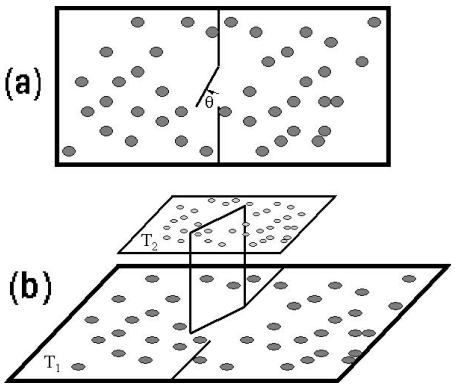

FIG. 1. (a) An illustration of the trap-door Maxwell demon. The hinged door between the two compartments can only open inside the left chamber so that fast-moving gaseous particles from the right chamber can move into the left one by lifting the door with significant collision impact. The average temperature of the two chambers is T_1, and those for the left and right chambers are T_L and T_R, respectively. (b) The trap door may be connected to another door in a third chamber with temperature T_2 such that the two doors have to move in unison.

simple trap door in Fig. 1(a) therefore fulfills the role of a Maxwell demon. In this work we shall simulate precisely such a realistic version of Maxwell's demons by employing molecular dynamics with the aim to probe the underlying nature of statistical mechanics at a microscopic scale.

In Fig. 1(a), two chambers of gaseous particles are separated by a solid wall with a built-in door which opens only inside the left chamber. Fast-moving particles are able to migrate from the right chamber to the left thanks to their ability to lift the trap door upon collisions, while their slow-moving counterparts are confined to their respective chambers due to lack of collision impact. The average temperature of the two chambers is T_1, and those for the left and right chambers are T_L and T_R, respectively. In Fig. 1(b), the trap door is connected to another door in a third chamber of temperature T_2 such that the two doors have to move in unison. The temperature of the trap door can therefore be tuned by adjusting T_2. For the purpose of comparison with the trap-door Maxwell demon, an alternative Maxwell demon made of a logic gate has also been devised. The logic gate is placed between two particle chambers examining the velocities of incoming particles v_{gas}. A particle in the right (left) chamber is only allowed to pass into the other chamber if v_{gas} is greater (smaller) than a preset threshold v_c. This particular setup of Maxwell's demon is termed the logic-gate demon.

II. THE MODEL

The system we have simulated contains two identical chambers, with a trap door placed in between. The gas molecules are hard dishes moving inside a two-dimensional space and colliding with each other. All collisions of gas molecules are energy and momentum conserving. After particle-wall collisions, the particle momentum reverses its component perpendicular to the wall. Geometrically, the trap door is a line segment of zero width impenetrable by the molecules. A spring with a force constant K_θ is placed between the trap door and the lower part of the middle wall. In the equilibrium position, the door is fully closed.

The Lagrangian of the system can be written as

$$L = \frac{1}{2}\sum_{i=1}^{N} m_{\text{gas}} v_i^2 + \frac{1}{2} I_{\text{door}} \dot{\theta}^2 - \frac{1}{2} K_\theta (\theta - \theta_0)^2 - V_{\text{int}}, \quad (1)$$

where v_i is the velocity magnitude of the ith gas particle, θ (θ_0) is the door angle (the equilibrium door angle), $\dot{\theta}$ is angular velocity, K_θ is the elastic constant of the door spring, m_{gas} and I_{door} are the mass of the gaseous particles and the momentum of inertia of the door, respectively, and V_{int} is the interaction potential energy among all rigid bodies in the system, which is constant except when particle-door collisions occur. The third term on the right-hand side of Eq. (1) describes the interaction between the spring and the trap door. Equations of motion for the particle velocities and the door angle θ are then derived from the Lagrangian. For instance, in the absence of collisions, the door angle $\theta(t)$ follows

$$\theta(t) = \theta_0 + [\theta(t_i) - \theta_0]\cos\left[\sqrt{\frac{K_\theta}{I_{\text{door}}}}(t - t_i)\right] + \dot{\theta}(t_i)\sqrt{\frac{I_{\text{door}}}{K_\theta}}\sin\left[\sqrt{\frac{K_\theta}{I_{\text{door}}}}(t - t_i)\right] \quad (2)$$

for $t \geqslant t_i$, where t_i denotes the starting time.

III. MOLECULAR DYNAMICS SIMULATION

In the simulation, the diameter (mass) of the gas particles is taken as the length (mass) unit and the Boltzmann constant k_B is set to unity. Various values for the chamber size and the trap door length have been experimented with, and a set of parameters is chosen as follows: the number of particles in each chamber, $N=30$; the size of each chamber, $S=200 \times 200$; the equilibrium door angle $\theta_0=0$; the length of the trap door, $R_{\text{door}}=50$; the momentum of inertia of the trap door, $I_{\text{door}}=0.2$; and the force constant $K_\theta=10$. Our simulation takes typically several hours using a standard Pentium 4 processor, and the fluctuation in the total energy of the system is kept below 10^{-10}.

The gas molecules are given random initial positions, and their velocities are initialized according to the Boltzmann distribution. The time evolution of the system of the molecules and the trap door is simulated by adopting the following algorithm: to minimize numerical errors, adaptable time steps are used. There are two kinds of time steps in this simulation. Our program iterates a main cycle which starts from t_0 to the end of simulation with a time step $\Delta t = 10^{-3}$. Within each cycle, the velocities and positions of all particles and the trap door are updated assuming no collision takes place; a subroutine is then called to examine collision events that may have been overlooked. Four types of collision events are involved: particle-particle collisions, particle-wall collisions, trap-door–wall collisions, and particle–trap-door collisions. Information of the previous step is recorded so

that we can restore a current state to one that precedes it. The collision criteria are (i) particle-particle collisions—the distance between two particles is less than the diameter of a particle; (ii) particle-wall collisions—the distance between particle and wall is less than the radius of a particle; (iii) trap-door-wall collisions: θ is smaller than 0 or larger than π; (iv) particle–trap-door collisions—the center of a particle enters the area near around the trap door as shown in Fig. 5 in Appendix B.

We take a particle-particle collision as an example. At the end of each time step, the center-of-mass distance between two particles is measured to determine whether a collision has taken place. If there is no collision, the simulation is carried on to the next time step. Otherwise, collisions need to be accounted for. In this case, the simulation is restored to the recorded previous state and the time step is reduced to $\Delta t' = 10^{-6}$. After the restoration, the program performs 10^3 steps using $\Delta t'$. It means one regular step is divided into 10^3 steps in a collision event. After the collision, the simulation returns to the main loop with the original time step Δt. If a three-body collision is to occur, our program records all the relevant information and pauses. However, such a three-body collision event has not been encountered in our system which is composed of 60 particles with a time step $\Delta t'$ as small as 10^{-6}.

We have carefully considered various collision events including particle-particle collisions, particle-wall collisions, and particle–trap-door collisions. Details on how these collision events are handled are explained in the Appendixes. Collisions between particles are described in Appendix A. For a particle-wall collision, the normal component of the particle's velocity reverses its direction while the tangential counterpart remains unchanged. Extreme care has been taken for particle–trap-door collisions, which are divided into two categories: events with particles colliding with the end of the trap door and those with particles colliding with the body of the trap door. Details are given in Appendix B.

IV. RESULTS AND DISCUSSION

Figure 2 displays simulation results of the system depicted in Fig. 1(a). The temperature of the gaseous molecules in the left or right compartment is determined by fitting their energy histogram to a Boltzmann distribution. The upper panel is the energy histogram of the gaseous molecules in the left compartment at a simulation time $t=2000$. The dashed line is the Boltzmann distribution with a temperature $T=2000$, and the temperature of the gas in the left compartment is thus determined. The middle panel shows the temperatures of the left and right compartments at various times between $t=0$ and 80 000. Despite the fluctuations, no visible temperature differentiation has been achieved by the trap door for the duration of the simulation. This reflects the fact that being hit frequently by the incoming particles the Maxwell demon is heated up, reaching thermal equilibrium with the gaseous particles, and loses therefore its designated functionality. This was pointed out precisely by Smoluchowski one century ago. The particle-door system is in thermal equilibrium and any temperature differentiation is in fact prohibited by the second law of thermodynamics. How exactly do Smoluchowski's fluctuations prevent the demon from establishing a temperature gradient between the two chambers? The lower panel in Fig. 2 reveals the underlying microscopic process. The two microscopic states shown in (a) and (b) of the panel are almost identical except that the velocities or momenta of the molecule and the trap door have opposite signs. The probabilities of the two microscopic states to occur are precisely the same. This is the so-called "principle of microscopic reversibility" [13] which leads to zero net heat flow between the two chambers.

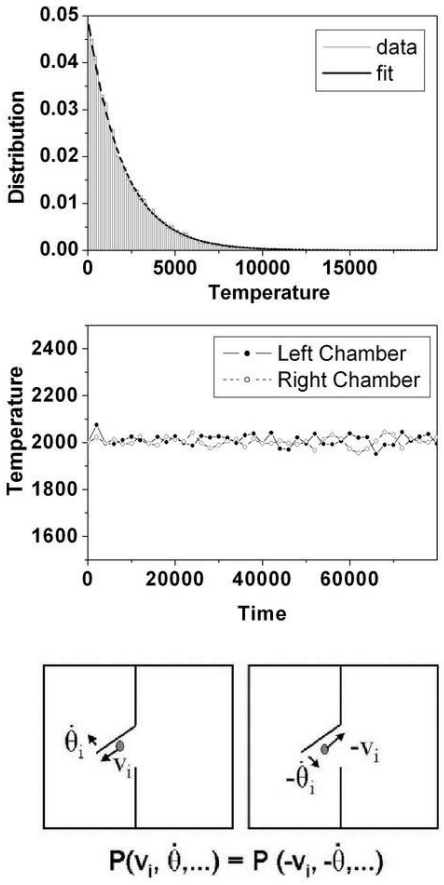

FIG. 2. Upper panel: the energy histogram of the gaseous particles in the left chamber at simulation time $t=2000$; the dashed line is the fitted Boltzmann distribution with $T=2000$. Middle panel: temperatures of the two chambers as a function of time given that the trap door is in a thermal equilibrium with the gaseous particles it separates; solid circles, left chamber; open circles, right chamber; solid and dashed lines are a guide for the eye. Lower panel: schematic illustration of the principle of microreversibility; (a) a molecule is moving from the right chamber to the left while the trap door rotates clockwise, and (b) the molecule is moving from the left to the right while the trap door moves counterclockwise. Distance (mass) is in the unit of the gas particle's diameter (mass), time is in the arbitrary unit, and temperature is evaluated by $T=\frac{1}{2}mv^2$ with k_B set to 1.

One important issue is whether it is ever possible for the Maxwell demon to perform its designated duty to direct the heat flows. One way for the Maxwell demon to achieve that end is to control Smoluchowski's fluctuations. As shown in

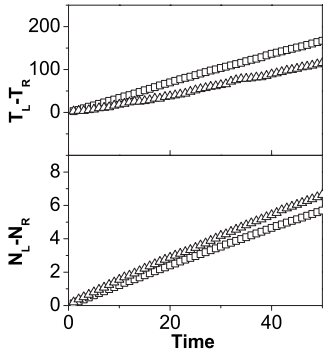

FIG. 3. Upper panel: temperature differences of the two chambers are plotted as a function of time after averaging over an ensemble of 10 000 trajectories; (a) the trap door demon (△), the temperatures are rescaled to keep their average constant (T_1 =2000), and the door temperature is rescaled to remain at T_2=10; (b) the logic-gate Maxwell demon (□), no temperature rescaling is needed. Lower panel: the number of particles in the left chamber as a function of time; (a) the trap door demon (△); (b) the logic-gate Maxwell demon (□) with a threshold velocity v_c=14.1. Each chamber initially contains 30 particles. The units are the same as in Fig. 2.

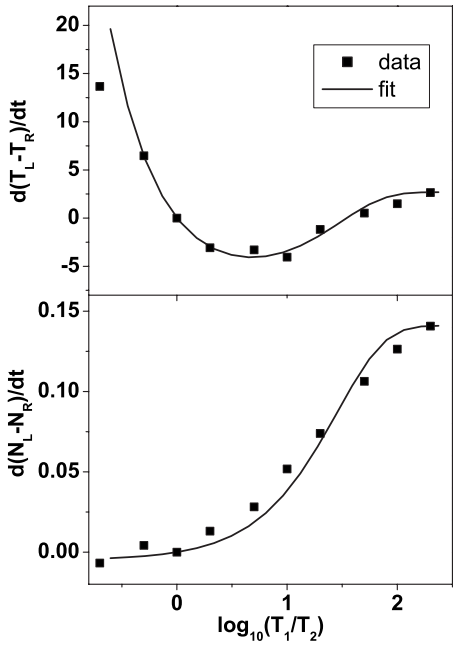

FIG. 4. Upper panel: the rate of change of the temperature difference between the left and right chambers in the trap door device, $d(T_L-T_R)/dt$, as a function of $\log_{10}(T_1/T_2)$; dots, simulation results; solid line, a smooth fit to the simulation results that employs an expression taking into account both the regular heat transfer in the direction of temperature gradient, $C(T_2-T_1)$, and the Feynman term $(e^{-\epsilon/T_1}-e^{-\epsilon/T_2})/\tau$, where C is a proportionality constant, τ is the characteristic time between two consecutive collisions, and ϵ is the energy required to lift the trap door [5]. Lower panel: the rate of change of the particle-number difference between the left and right chambers in the trap door device, $d(N_L-N_R)/dt$, as a function of $\log_{10}(T_1/T_2)$; dots, simulation results; solid line, a smooth fit to the simulation results with Feynman's expression $D(e^{-\epsilon/T_1}-e^{-\epsilon/T_2})/\tau$. C=0.0033, τ=0.104, ϵ=70, and D=0.0152. Data displayed are averaged by an ensemble of 2000 trajectories. The units are the same as in Fig. 2.

Fig. 1(b), the trap door can be connected rigidly to another particle-colliding door in a third compartment such that the two doors have to move in unison; therefore, the door temperature can be manipulated by varying the temperature of the third chamber. In other words, Smoluchowski's fluctuations of the demon can be tuned by controlling the temperature of the third compartment, T_2. In the simulation, the total kinetic energy of the gaseous particles in the lower box is kept constant. If the temperature of the door is kept sufficiently low by external means, the simple trap-door device in Fig. 1(b), which is no longer strictly an equilibrated close system, can actually function as designed; i.e., it can work as a Maxwell demon. In this case, Smoluchowski's fluctuations are reduced. Shown in the upper panel of Fig. 3 is the temperature difference between the two chambers as a function of time after averaging over an ensemble of 10 000 individual trajectories (30 particles in each chamber). The trap door is kept at a much lower temperature, T_2=10, than the initial temperature of the particle chambers, T_1=2000. As collisions in the simulation tend to cool the particles of the lower two chambers, their average temperature is rescaled to stay constant. The lower panel of Fig. 3 displays the number of particles in the left chamber as a function of time.

Maxwell's demon was originally a perceived being similar to a logic gate sitting between two chambers. Its function that our trap door device has now assumed is quite clear-cut: the particles in the right chamber with speeds above a threshold (e.g., v_c=14.1) are allowed to move to the left, while the particles in the left chamber with speeds below the threshold are allowed to move to the right. For the purpose of comparison with our trap-door demon, we also display in Fig. 3 results from the logic-gate demon using squares (averaged over an ensemble of 10 000 trajectories). Very similar behavior is found for the two kinds of demons.

Figure 4 summarizes various factors that affect the ability of the Maxwell demon to create interchamber temperature differences. All data points in the figure are calculated by averaging over 2000 individual trajectories. The origin in the upper panel represents the result previously shown in Fig. 2 where the two chambers are at thermal equilibrium with the trap door and no temperature differentiation happens. If the trap door is cooled to a lower temperature, initially a temperature difference is caused by the cooling effect of the door—i.e., $T_L-T_R<0$. If the temperature of the trap door T_2 is lowered further, the simple Maxwell demon starts to exhibit its designed capability to modulate interchamber heat flows. At $\log_{10}(T_1/T_2)$=1.5, the cooling effect of the trap door becomes overwhelmed by its designed demon effect, and therefore, the temperature difference between the left and right chambers is reversed—i.e., $T_L-T_R>0$—as the door temperature T_2 decreases. In the limit of zero door temperature, the device acts as the perfect Maxwell demon. On the other hand, if the trap door is heated up to a higher temperature, it can only serve as a heater by raising the left chamber temperature and no reverse temperature difference $(T_L-T_R<0)$ is found to exist, contrary to the the prediction Feynman made for his ratchet-and-pawl system [5]. The

simulation results in Fig. 1(a) have been fitted with an expression that takes into account both the regular heat transfer in the direction of the temperature gradient, $C(T_2-T_1)$, and the Feynman term $(e^{-\epsilon/T_1}-e^{-\epsilon/T_2})/\tau$, where C is the proportionality constant in Fourier's law of heat conduction, τ is the characteristic time between two consecutive collisions, and ϵ is the energy required to lift the trap door [5]. For $T_1=T_2$, each chamber has 30 particles—i.e., $N_L=N_R=30$. As T_2 is lowered, more and more particles are found in the left chamber at long times. If the trap door is warmer than the gaseous particles, the trend is reversed; i.e., a smaller amount of particles are found in the left chamber. The rate of change of the particle-number difference between the left and right chambers in the trap door device, $d(N_L-N_R)/dt$, is shown as a function of $\log_{10}(T_1/T_2)$ in the lower panel of Fig. 4, and a smooth fit with Feynman's expression $(e^{-\epsilon/T_1}-e^{-\epsilon/T_2})/\tau$ is also given. We conclude that it is much easier for the trap door device to create a density gradient provided that its temperature T_2 is different from the average temperature T_1 of the two lower chambers in Fig. 1(b).

In their pioneering work [7] Skordos and Zurek explored via numerical simulation quite a few issues that have been discussed here, such as the cooled trap door as a rectifier. Another remarkable work that only recently came to our attention is modeling and simulation of Brownian refrigerators by Van den Broeck and Kawai [14]. A Brownian motor that is normally driven by a temperature gradient can also become a refrigerator upon loading. The temperature gradient created by a Brownian refrigerator, however, is different from that created by the Maxwell demon discussed here as the former is a form of negative feedback by the original equilibrium system upon perturbation [14].

In summary, a simulation has been performed to reveal the detailed dynamics and statistical behavior of a Maxwell demon in the presence of equilibrium or nonequilibrium baths. The second law of thermodynamics dictates that no temperature differentiation can happen when the trap door and the chamber particles are in thermal equilibrium. This is confirmed by our molecular dynamics simulation of the trap door Maxwell demon. The temperature of the trap door can be controlled in order to tune Smoluchowski's fluctuations and to further manage the role of the Maxwell demon. This study reveals in great detail the intricacies among the second law of thermodynamics, Maxwell's demon, and Smoluchowski's trap door.

ACKNOWLEDGMENTS

This work was supported by the Hong Kong Research Grants Council (Grants Nos. HKU 7064/06P and HKU 7127/05E) and Committee on Research and Conference grants (CRCG) of University of Hong Kong.

APPENDIX A: COLLISIONS BETWEEN PARTICLES

The phase-space coordinates (positions and velocities in a Cartesian system) of particle 1 immediately before and after a collision event are denoted as $(x_1,y_1,\dot{x}_{1i},\dot{y}_{1i})$ and $(x_1,y_1,\dot{x}_{1f},\dot{y}_{1f})$, respectively. Similarly for particle 2, we have $(x_2,y_2,\dot{x}_{2i},\dot{y}_{2i})$ and $(x_2,y_2,\dot{x}_{2f},\dot{y}_{2f})$. Changes in the particle velocities upon a collision event between particles 1 and 2 are quantified by

$$\begin{pmatrix} \dot{x}_{1f} \\ \dot{y}_{1f} \\ \dot{x}_{2f} \\ \dot{y}_{2f} \end{pmatrix} = \begin{bmatrix} A^2 & -AB & B^2 & AB \\ -AB & B^2 & AB & A^2 \\ B^2 & AB & A^2 & -AB \\ AB & A^2 & -AB & B^2 \end{bmatrix} \begin{pmatrix} \dot{x}_{1i} \\ \dot{y}_{1i} \\ \dot{x}_{2i} \\ \dot{y}_{2i} \end{pmatrix}, \quad \text{(A1)}$$

where

$$A \equiv \sin\alpha = \frac{y_2-y_1}{r},$$

$$B \equiv \cos\alpha = \frac{x_2-x_1}{r},$$

$$r \equiv \sqrt{(x_2-x_1)^2+(y_2-y_1)^2}. \quad \text{(A2)}$$

Here α is the angle formed by the x axis and the line which goes through the centers of the two particles.

APPENDIX B: PARTICLE–TRAP-DOOR COLLISIONS

The dashed line in Fig. 5 is the trajectory of the particle center of mass that is closest to the trap door. The area enclosing the trap door with a width equal to the diameter of the particles (inside the dashed line) is divided into four parts, labeled A, B, C, and D, respectively. Collisions are expected whenever the particle center of mass enters this area during simulation.

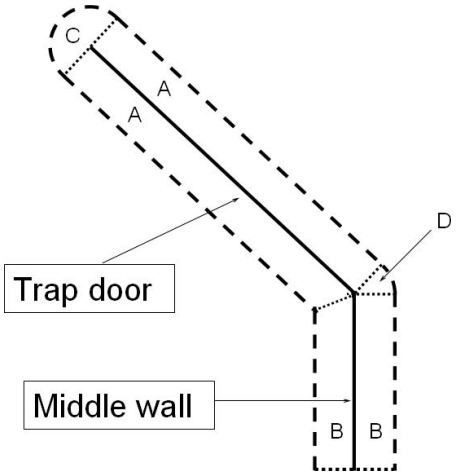

FIG. 5. A collision occurs when the center of mass of a particle reaches the area labeled by a, b, c, d, e, or f.

Collision events can be classified into four categories according to the specific area accessed by the particle center of mass: (i) for A, a collision between a particle and the body of the trap door; (ii) for C, a collision between the particle and the end of the trap door; (iii) for B, a collision between the particle and the center wall; (iv) for D, a collision between the particle and the joint of the trap door and the middle wall.

As shown in Fig. 6, the angle of the trap door in a polar coordinate system is labeled as θ and the coordinates of a gas

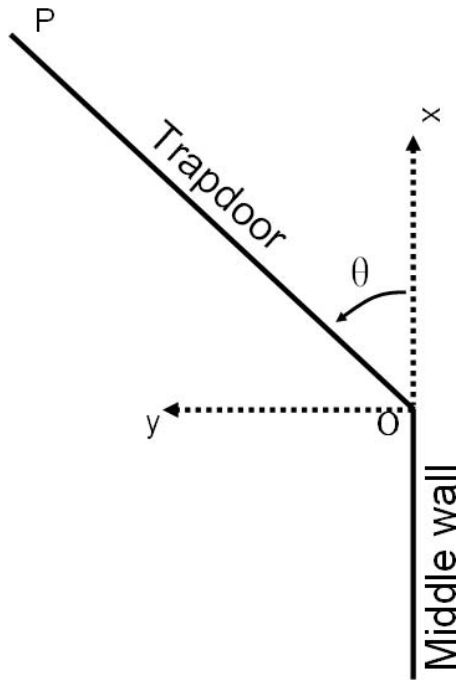

FIG. 6. The range of the angle θ would be $(0,\pi)$.

particle (x,y). The angular velocity of the trap door and the particle's velocity immediately after the collision, $\dot{\theta}_f$ and $(\dot{x}_f,\dot{y}_f)$, respectively, can be derived from Newton's laws

$$\dot{\theta}_f = \dot{\theta}_i + \frac{\partial_\theta h}{I_{\text{door}}}\Delta P, \tag{B1}$$

$$\dot{x}_f = \dot{x}_i + \frac{\partial_x h}{m_{\text{gas}}}\Delta P, \tag{B2}$$

$$\dot{y}_f = \dot{y}_i + \frac{\partial_y h}{m_{\text{gas}}}\Delta P. \tag{B3}$$

Here $\dot{\theta}_i$ and $(\dot{x}_i,\dot{y}_i)$ are the corresponding velocities immediately before the collision and ΔP is the impulse upon the collision:

$$\Delta P \equiv -\lim_{\delta t\to 0}\int_{t_i}^{t_i+\delta t}\left.\frac{\partial V_{\text{int}}}{\partial h}\right|_{h=R} dt$$

$$= -2\frac{\partial_\theta h\dot{\theta}_i + \partial_x h\dot{x}_i + \partial_y h\dot{y}_i}{\dfrac{(\partial_\theta h)^2}{I_{\text{door}}} + \dfrac{(\partial_x h)^2}{m_{\text{gas}}} + \dfrac{(\partial_y h)^2}{m_{\text{gas}}}}, \tag{B4}$$

where t_i is the time immediately before the collision. Equations (B1)–(B4) are valid for the aforementioned two categories.

1. Collisions with the trap-door body

In this case, h is distance between the particle center of mass and the body of the trap door. Various quantities h, $\partial_\theta h$, $\partial_x h$, and $\partial_y h$ can be be expressed as (see Fig. 6)

$$h = x\sin\theta - y\cos\theta + R,$$

$$\partial_\theta h = x\cos\theta + y\sin\theta,$$

$$\partial_x h = \sin\theta,$$

$$\partial_y h = -\cos\theta, \tag{B5}$$

where R is the radius of the particle.

2. Collisions with the trap-door edge

In this case, h is defined as the distance between the particle center of mass and the trap-door edge. Therefore, we have

$$h = \sqrt{(x - R_{\text{door}}\cos\theta)^2 + (y - R_{\text{door}}\sin\theta)^2} - R,$$

$$\partial_\theta h = \frac{R_{\text{door}}(x\sin\theta - y\cos\theta)}{R},$$

$$\partial_x h = \frac{x - R_{\text{door}}\cos\theta}{R},$$

$$\partial_y h = \frac{y - R_{\text{door}}\sin\theta}{R}. \tag{B6}$$

[1] J. C. Maxwell, *Theory of Heat* (Longmans, London, 1871).
[2] W. Thomson, Nature (London) **9**, 441 (1874).
[3] Y. Zhao, C. C. Ma, L. H. Wang, G. H. Chen, Z. P. Xu, Q. S. Zheng, Q. Jiang, and A. T. Chwang, Nanotechnology **17**, 1032 (2006); Y. Zhao, C. C. Ma, G. H. Chen, and Q. Jiang, Phys. Rev. Lett. **91**, 175504 (2003); C. C. Ma, Y. Zhao, C. Y. Yam, G. H. Chen, and Q. Jiang, Nanotechnology **16**, 1253 (2005).
[4] M. v. Smoluchowski, Phys. Z. **13**, 1069 (1912).
[5] R. P. Feynman, R. B. Leighton, and M. Sands, *The Feynman Lectures on Physics I* (Addison-Wesley, Reading, MA, 1963), Chap. 46.
[6] K. Zhang and K. Zhang, Phys. Rev. A **46**, 4598 (1992).
[7] P. Skordos and W. Zurek, Am. J. Phys. **60**, 876 (1992).
[8] P. A. Skordos, Phys. Rev. E **48**, 777 (1993).
[9] C. Jarzynski and O. Mazonka, Phys. Rev. E **59**, 6448 (1999).
[10] P. Meurs, C. Van den Broeck, and A. Garcia, Phys. Rev. E **70**, 051109 (2004).
[11] M. O. Magnasco and G. Stolovitzky, J. Stat. Phys. **93**, 615 (1998).
[12] C. Van den Broeck, R. Kawai, and P. Meurs, Phys. Rev. Lett. **93**, 090601 (2004); C. Van den Broeck, P. Meurs, and R. Kawai, New J. Phys. **7**, 10 (2005).
[13] R. C. Tolman, *The Principles of Statistical Mechanics* (Dover, New York, 1979).
[14] C. Van den Broeck and R. Kawai, Phys. Rev. Lett. **96**, 210601 (2006).